revista principia 30 anos
Revelando e explicando o futuro
ISSN 2447-9187

https://doi.org/10.18265/2447-9187a2026id9048
ORIGINAL ARTICLE

SUBMITTED May 14, 2025
APPROVED September 29, 2025
PUBLISHED ONLINE January 22, 2026
FINAL FORMATTED VERSION July 14, 2026
ASSOCIATE EDITOR
Prof. Dr. Arthur Willian de Lima

Analysis of the C260 brass after mechanical forming and annealing

Douglas Luiz da Cruz [1] *
Matheus José Cunha de Oliveira [2]
Cristian Pohl Meinhardt [3]

[1] douglascruzjf@gmail.com
[2] matheus.oliveira@ifsudestemg.edu.br
Instituto Federal de Educação, Ciência e Tecnologia do Sudeste de Minas Gerais (IF SUDESTE MG), Juiz de Fora, Minas Gerais, Brazil

[3] cristianmeinhardt@unipampa.edu.br
Universidade Federal do Pampa (UNIPAMPA), Alegrete, Rio Grande do Sul, Brazil

* *Corresponding author.*

ABSTRACT: Copper alloys such as brass are widely employed in various industrial sectors due to their characteristics such as corrosion resistance and formability. Among the processes used to manufacture parts made with such alloys, processes such as deep stamping or inlaying and stretching stand out. Such mechanical forming processes require heat treatments such as annealing, to achieve specific properties in the resulting material. Therefore, this work aimed to evaluate the mechanical behavior of C260 brass when subjected to mechanical shaping (blanking and stretching) and annealing heat treatment. For this, a script clipping of an ammunition component was used, sampling each step from the raw material to the cup shape, with the latter being divided into different regions, to understand the processes. Metallographic tests were carried out to evaluate the microstructure and determine grain size and Vickers microhardness. The grain size data were treated statistically, thus making it possible to judge the significance of each microstructure alteration. Thus, it was possible to observe that the mechanical forming steps promoted strain hardening, unlike the annealing. However, a difference in behavior was noted in two different regions of the cups: the wall region showed significant microstructural and hardness variations, unlike the bottom region. The percentage of cold work parameters was identified as responsible for these differences both for recrystallizations to occur, as well as for the resulting microstructure and consequent hardness. Finally, the evaluation of the data referring to the raw material confirmed the fulfillment of its technical requirements.

Keywords: copper alloy; heat treatment; metallurgy; microstructure.

Análise do latão C260 após conformações mecânicas e recozimento

RESUMO: *Ligas de cobre como o latão são muito utilizadas nos mais variados ramos da indústria devido a características como resistência à corrosão e conformabilidade. Entre os processos utilizados para a fabricação de peças com essas ligas, destacam-se a estampagem profunda (ou embutimento) e o estiramento. Tais processos de conformação mecânica requerem a utilização de tratamentos térmicos como o recozimento, a fim de se obter propriedades* *específicas no material resultante. Portanto, o presente trabalho teve como objetivo avaliar o comportamento mecânico do latão C260 quando submetido a tratamento térmico de conformação mecânica (embutimento e estiramento) e recozimento. Para isso, foi utilizado um recorte de roteiro de um componente de munição, retirando-se, passo a passo, amostras desde a matéria-prima até o formato de copo, sendo este último dividido em diferentes regiões, para entender os processos. Foram realizados ensaios metalográficos para a avaliação microestrutural, permitindo determinar o tamanho do grão e a microdureza Vickers. Os dados de tamanho de grão foram tratados estatisticamente, possibilitando julgar a significância de cada alteração microestrutural. Assim, foi possível observar que as etapas de conformação mecânica realmente endureceram o material, diferentemente do recozimento. Porém, notou-se diferença de comportamento em duas regiões distintas dos copos: a região da parede apresentou significativas variações microestruturais e de dureza, diferentemente da região do fundo. O parâmetro "percentual de trabalho a frio" foi identificado como responsável por essa diferença, tanto para que ocorram recristalizações quanto para a microestrutura resultante e consequente dureza. A avaliação dos dados referentes à matéria-prima confirmou o atendimento aos seus requisitos técnicos.*

Palavras-chave: *liga de cobre; metalurgia; microestrutura; tratamento térmico.*

1 Introduction

Blanking is a sheet metal forming process characterized by a punch moving against another tool called a matrix containing the sheet metal. The geometry of the punch/die set is responsible for the new shape of the sheet metal (Hirt *et al*., 2005).

Brass is a copper–zinc (Cu–Zn) solid-solution alloy that combines the corrosion resistance and formability of copper with higher mechanical strength. It is widely used to manufacture complex shapes – through deep drawing, for instance –, because it hardens slowly, tolerates stress well, and fractures only at high strains (Brooks, 1982). Consequently, this alloy is of great importance to the metalworking industry. These characteristics, combined with its aesthetic appeal, make brass used in several areas, such as decoration, electrical, automotive, military, civil construction, oil and gas (Barbosa, 2014).

The deformation processes used to obtain certain application characteristics in the final product require the use of heat treatment. This aims to restore the material's physical-mechanical properties to their previous levels. Such treatment is called annealing. The metallurgical phenomena characteristic of the annealing of metallic alloys and their relationship with the microstructure of the deformed metal have been objects of study for many years (Moreira, 2015).

The present work focuses its analysis on a specific brass alloy, the binary brass C260, also known as "cartridge brass" due to its widespread application in the manufacturing of ammunition components. It is a single-phase alloy; therefore, its microstructure consists only of α phase (copper with zinc in solid solution), which is highly suitable for stamping processes due to its good mechanical resistance and excellent ductility. The proposed analysis seeks to elucidate the behavior of Cu–Zn 30 brass, as it is also known, through mechanical forming and heat treatment in a cutout of the manufacture script of an ammunition component.

Section 2 presents the bibliographic review, covering fundamental concepts regarding stamping, deep drawing, stretch forming processes, annealing heat treatments, and the specific properties of the C260 brass alloy. Section 3 details the experimental methodology, describing the planning of the mechanical forming and heat treatment routes, specimen preparation, and the procedures for metallographic analysis and Vickers microhardness testing. Section 4 is dedicated to the results and discussion, analyzing the microstructural and mechanical evolution of the alloy after each processing step. Finally, Section 5 synthesizes the main conclusions derived from the study, followed by Section 5.1, which addresses the limitations of the research and outlines perspectives for future work.

2 Bibliographic review

Stamping comprises a set of various operations performed on blank metal sheets, which aim to transform them geometrically, resulting in folds, cavities, protrusions, wedges and holes. These deformations occur in the solid state, causing the material to flow within the plastic regime. One of the positive points of stamping is the reduced waste and low generation of scrap material.

Plastic deformation, generally cold, is carried out using stamping presses equipped with tools known as dies. As a result of the characteristics of this sheet metal forming process, various methods have been developed over the years, bringing together specialists from each process for their respective application. Along with this diversification of methods, several parameters are specific to each process. Such as tooling angles and radii, clearance, operating speed, roughness and strength, in addition to the physical-mechanical properties of the raw material used in the process.

Inlay or deep drawing is a stamping process used to transform flat sheets into three-dimensional and deep parts of different shapes, such as cups, pans, capsules, car body components and metal packaging. The tooling used in these operations consists of a punch, a die and a blank holder. During deep drawing, a force is exerted on the central region of the blank, forcing it towards the matrix cavity and pulling the flap region in the same direction, which results in a gradual reduction in the circumference of the disc in this region. This effort generates tensile and compressive stresses in several regions. Tensions act in the flap region, which touches the concentric circles to the central region, called circumferential compression and which tend to wrinkle the sheet. To avoid this, the plate press must exert a compressive stress, called holding pressure. This pressure should only be necessary to avoid the appearance of wrinkles, thus allowing the movement of the disc flap towards the central region. Stretch forming is characterized by a state of biaxial traction, where traction forces are applied in order to stretch the material over a tool or block (die), thus defining the contour of the part and a reduction in the thickness of the material. The springback effect is almost completely eliminated due to a higher percentage of plastic deformation caused by the tensile force, thus reducing residual stresses. However, only in materials with high ductility values, can large stretching deformations be obtained due to the predominance of tensile stresses (Grigoras *et al*., 2024).

The stresses generated in various manufacturing processes, such as casting, mechanical forming and even machining, induce structural changes in materials. These modifications alter mechanical properties of the materials that pass in this way, not always corresponding to the application requirements of the manufactured parts (Merayo; Rodríguez-Prieto; Suárez, 2021). Consequently, it is often necessary to subject them to heat treatments that aim to readapt such properties, which can be considered the most common method for achieving the desired material characteristics.

The term annealing is used generically to describe a set of heat treatments performed to relieve or remove residual stresses, decrease hardness, improve ductility and toughness, as well as produce a specific microstructure. Basically, it consists of heating the metal to a specific temperature, maintaining that temperature for a duration known as "soaking time," and then cooling the material to room temperature. The importance of controlling time in this heat treatment is critical, considering that there are temperature gradients during heating and cooling in the material. Large rates of temperature variation can lead to warping or even cracking. The actual annealing time must be estimated in a way that allows for all necessary transformations to occur. Temperature is another very important parameter, which can accelerate annealing by increasing it, considering the diffusion processes normally involved (Birch *et al*., 2024).

Commonly referred to as "cartridge brass," the C260 single-phase copper alloy has a yellowish color and is highly recommended for various forming processes, particularly stamping and deep drawing, as it presents the most favorable combination between mechanical strength and ductility. Depending on the environment in which it is being used, it may be susceptible to dezincification problems (Barbosa, 2014). In addition to the manufacture of ammunition components, Brass UNS C26000 – as it is commercially known – has diverse applications, such as radiator cores and tanks, lamp fixtures, latches, locks, hinges, plumbing accessories, pins, rivets (ASM International, 1992). Thus, this work aimed to demonstrate the mechanical behavior and microstructure characterization of the C260 brass alloy under the effect of mechanical deformation and heat treatment, while also evaluating the initial state of the material.

3 Method

Aiming to study the behavior of the microstructure of Brass C260 during the mechanical forming process and during annealing, properties such as hardness and grain size of the raw material and samples of the material were evaluated after each of the four stages of the fabrication route for an ammunition component. Based on the experimental results, this study aimed to establish the relationship between the microstructure and the physical-mechanical properties of the alloy.

For specimen preparation, five 70/30 brass blanks were selected, which are typically used as raw material in cartridge manufacturing. One blank was separated immediately, while the remaining four underwent cold deep drawing in a hydraulic press, followed by alkaline degreasing, after which one cup sample was extracted. The three remaining cups were then annealed in a trolley furnace and subsequently pickled, where another cup sample was taken. The two remaining cups were subjected to cold stretching in a hydraulic press, followed by alkaline degreasing; and one more cup was removed. The final cup underwent a second annealing in the same furnace. The selected samples (cups and the blank) were coded for identification and their dimensions measured using a Mitutoyo digital caliper. Selected samples were sectioned to extract specimens for microhardness testing and metallographic analysis, according to relevant standards. The sampling and specimen preparation procedures described above are illustrated in the flowchart in Figure 1.

ISSN 2447-9187

Figure 1 ▶
Descriptive planning used in the work.
Source: elaborated by the authors

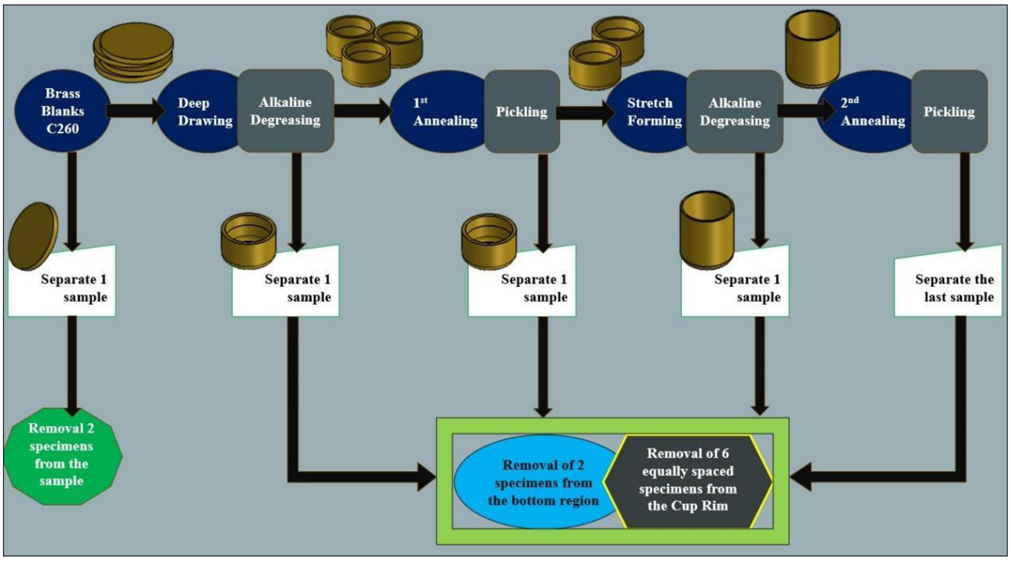

The flowchart in Figure 2 summarizes the experimental methods and analysis of the results.

Figure 2 ▶
Flowchart of the tests carried out.
Source: elaborated by the authors

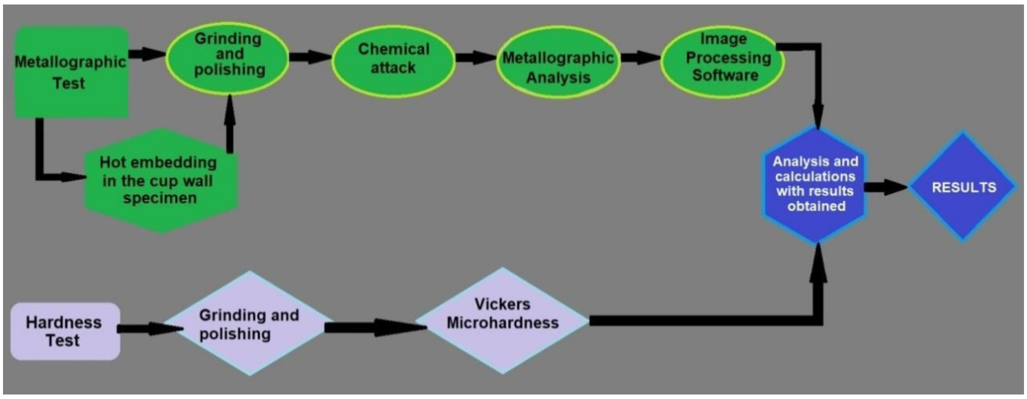

The blanks underwent a deep drawing process in a hydraulic press with a capacity of 2,200 tf from the Hidralmac brand. Drawing tallow was applied as a lubricant to both the punch surface and the blank. The cups subjected to alkaline degreasing were subsequently annealed in a Jung trolley furnace, where the samples were charged at room temperature and heated for approximately 1 hour until reaching 600 °C. The samples were held at this temperature for 25 minutes, then removed from the furnace and allowed to air-cool inside the still-hot trolley. Subsequently, the cups were pickled and subjected to stretching in a hydraulic press with a capacity of 150 tf from the Hidralmac brand. Again, drawing tallow was used as a lubricant on the punch surface as well as on the inside and outside of the cup.

After cleaning, the cups were charged at room temperature into the Jung trolley furnace and heated for approximately 30 minutes until reaching 550 °C, where they remained for 20 minutes before being removed and left to air-cool inside the still-hot trolley.

Figure 3 illustrates the preparation of the specimens obtained from the blanks. Two specimens were extracted from the sample, a small square with a side of 20 mm to carry out the metallography (3a) and another square with a side of 30 mm to obtain the hardness profile (3b).

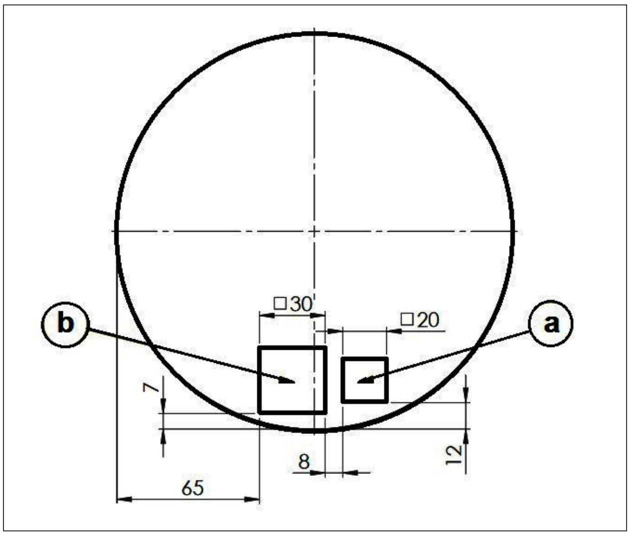

Figure 3 ▶
Test specimens originating from blanks: (a) Metallography; (b) Microhardness.
Source: elaborated by the authors

Subsequently, two specimens were removed from the cup bottom region (Figure 4a): a square with a side of 20 mm to carry out the metallography and another square with a side of 30 mm to obtain the hardness profile. Finally, six equally spaced specimens, with a width of 20 mm, were removed from the cup rim (wall), one for metallography and the others for obtaining the hardness profile, as shown in Figure 4b. Due to variations in cup height resulting from the processing steps, the sampling region for these wall specimens was standardized with its lower limit set at 25 mm from the lowest point of the cup edge.

Figure 4 ▼
Sample sections: (a) Bottom region; (b) Wall region.
Source: elaborated by the authors

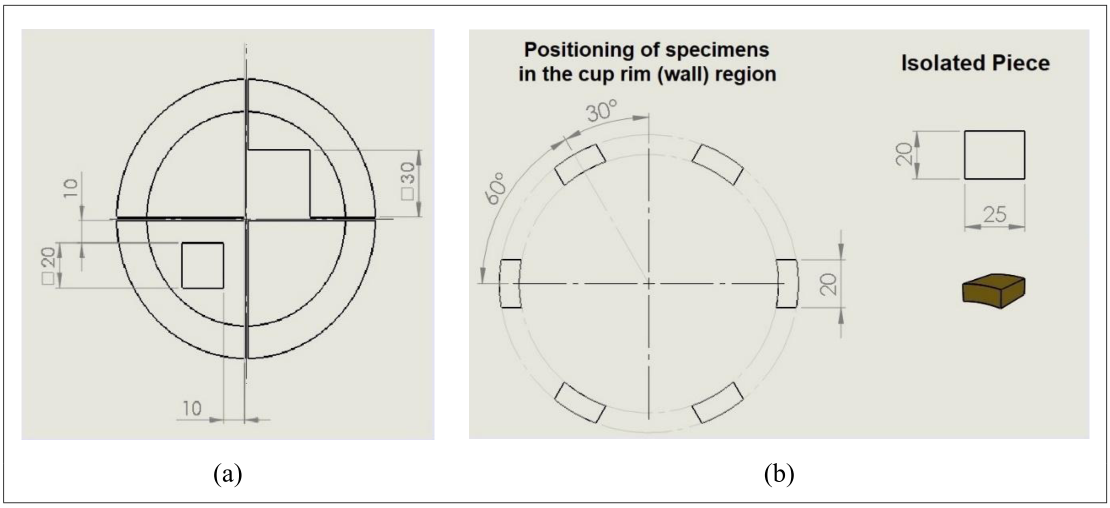

The metallographic preparation was carried out according to the procedures recommended by ASTM E3-11 (ASTM International, 2017) as follows: hot mounting in a Fortel brand press, model EFD 30, applied only to the samples taken from the cup walls. Subsequently, grinding was performed together with the other specimens in the following sequence of 80, 600, 800, 1,200 and 1,500 grit sandpapers, followed by polishing on felt cloth with diamond pastes of 3 and 1 µm grain size, and final finishing with 0.3 µm alumina. A Teclago metallographic grinder, model PL02 ED, and a double polisher, Arotec, model PL 02, were used for these operations. The specimens were also washed with 99% isopropyl alcohol and dried with a heated air jet, before being etched for 3 seconds with 100% Nitric acid (HNO_3) using a cotton pad.

To analyze the respective grain sizes, the linear intercept method or Heyn was applied, in accordance with the ASTM E112-10 (ASTM International, 2010) standard with the ImageJ software. The total length of the test lines divided by the count result was adopted as the average grain size. Subsequently, this value was used to calculate the ASTM grain size (G), according to Equation 1.

$$G = \left(6{,}643856.\log\left(P_L\right)\right) - 3{,}288 \quad (1)$$

Where:

P_L: number of grain boundary intersections per unit of test line length, in mm^{-1} according to ASTM E112 (ASTM International, 2010).

The obtained results also underwent a Shapiro-Wilk test using the PAST statistical software to assess whether the data distribution was normal or Gaussian distribution for the purpose of comparing the means. Subsequently, a comparison of the average grain sizes was performed using Tukey's Test, this time using the R_{studio} software. This test aimed to identify the significance of grain size variations between different processing operations. For the metallographic test, the samples were grinded in the following sequence of 80, 600, 1,500 grit sandpaper, followed by polishing on felt cloth with 1-µm alumina. A Teclago metallographic grinder, model PL02 ED, and a double polisher, Arotec, model PL 02, were used for grinding and polishing operations. The pieces were also washed with 99% isopropyl alcohol and dried with a heated air jet, being subsequently tested in a Vickers Digital Microhardness Tester, Shimadzu, model HMV - G 21 ST, with a load of 0.2 kgf, penetration for 5 seconds and magnification of 40 times.

Five indentations were made on the specimens from the blank and the bottom region (Figure 5a) and 1 indentation in each of the five squares on the edge of the cup (Figure 5b). Figure 5 illustrates the reference measurements for these indentations in both cases. To improve the support during the wall hardness tests, given the specimen's shape, a high-hardness steel (AISI H13) was employed, with a radius matching that of the punch used to form the inner diameter of the cups.

Figure 5 ▼ Distribution of hardness test indentations: (a) Bottom region and Blank; (b) Wall region. *Source: elaborated by the authors*

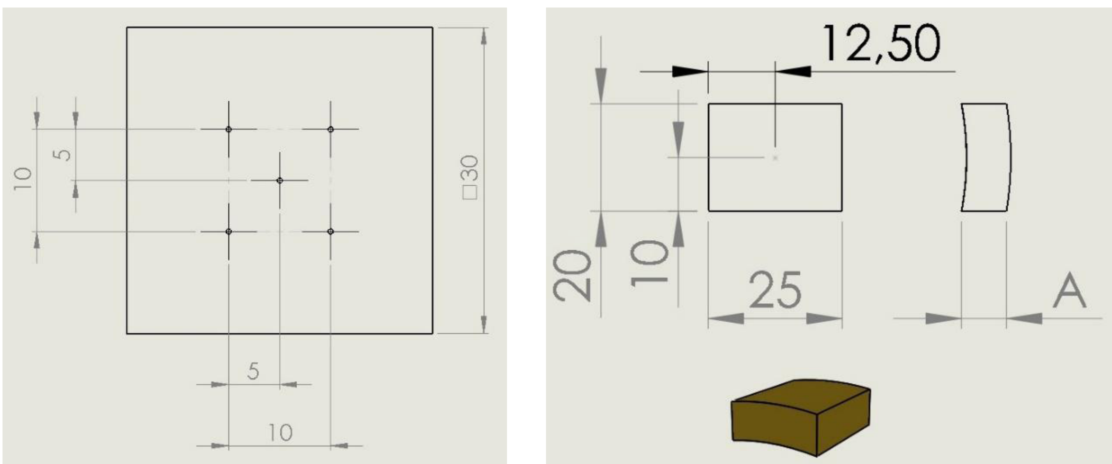

(a) (b)

4 Results and discussion

Figure 6 shows a diagram of the dimensions obtained using a digital caliper and Table 1 provides the step-by-step values for the cup-shaped samples.

Figure 6 ▼
Sample dimensions:
a) Blank; b) Cup shape.
Source: elaborated by the authors

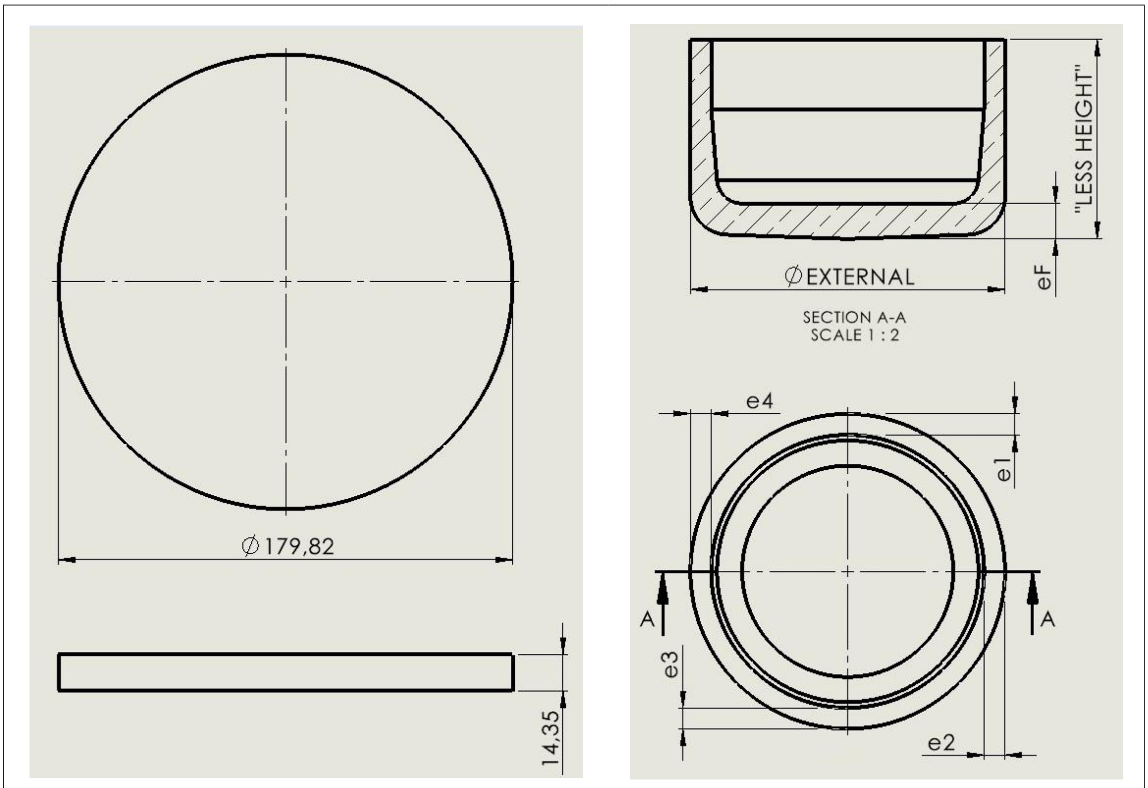

(a) (b)

Table 1 ▶
Table dimensions in mm of the cup-shaped samples.
Source: research data

Operation	Thickness (e) (mm)						Ø External (mm)	Lesser height (mm)
	e1	e2	e3	e4	Av.	eF		
Deep Drawing	8.8	8.3	8.6	8.6	8.6	14.10	124.8	80.5
1st Annealing	8.4	8.4	8.4	8.5	8.4	14.15	124.85	80.2
Stretch forming	4.5	4.7	4.9	4.5	4.7	14.08	117.05	140.2
2nd Annealing	4.4	4.4	4.5	4.5	4.5	14.10	117.05	143.2

Based on these values, it was possible to calculate the percentage of cold work (%CW) for each stage, using Equation 2, resulting in the data presented in Table 2.

$$\%CW = \left(\frac{A_0 - A}{A_0} \right) X\,100 \tag{2}$$

Where:

A_0: Initial cross-sectional area;

A: Final cross-sectional area.

ISSN 2447-9187

Table 2 ▶
Percentage of cold work for each stage of the process.
Source: research data

Operation		R external (mm)	R internal (mm)	E avg (mm)	Area (mm²)	Cold work (%CW)
Blank		89.91	-	14.35	7459.69	-
Deep Drawing	1st ring	65.00	54.07	10.93	4088.58	45.19
	2nd ring	62.41	53.91	8.50	3106.29	24.03
Stretch forming		58.53	53.98	4.60	1608.10	48.23

The deep drawing die comprises two sequential rings. The design parameters of the first ring were utilized in the calculations, as measuring the cup immediately after passing through this ring is not feasible. Therefore, the post-deep drawing cold work percentage (%CW) represents the cumulative effect of both rings. The external radius (R_{ext}) and average values for the second ring, as well as for the stretching process, are derived from the mean dimensional measurements of the cups that were hardened and immediately annealed after each operation.

It is evident that the deep drawing operation yields the highest cold work percentage.

Micrographs at 100× magnification (Figures 7 and 8) reveal the α-phase matrix of the brass and confirm the presence of mechanical or annealing twins in all samples. This is consistent with the predictions by Humphreys & Hatherly (2004) and Birch *et al*. (2024) for materials possessing low stacking fault energy.

Figure 7 ▶
Micrograph of the C260 brass blank.
Source: elaborated by the authors

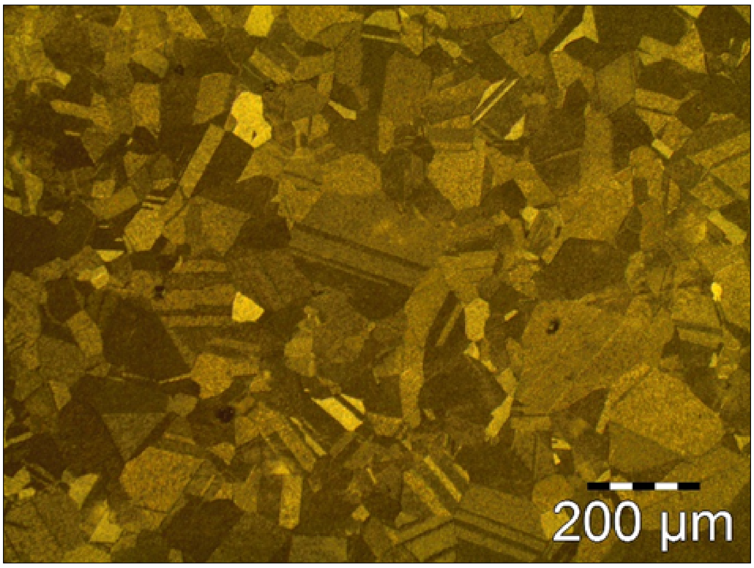

The Blank micrograph (Figure 7) demonstrates a predominance of equiaxed grains, which are randomly oriented. This lack of preferred orientation or texture prevents anisotropic behavior and subsequent forming defects, such as wall thinning or earing. Based on this analysis, it is possible to state that the technical requirements of the blank (rolled and annealed) were met, as new grains were nucleated through the recrystallization process. Figure 8 represents the stages deformed in a cup shape, with 8a, 8c, 8e and 8g the bottom regions and 8b, 8d, 8f and 8h the wall regions.

ISSN 2447-9187

Figure 8 ►
Micrograph of the C260 brass samples: bottom regions 8a, 8c, 8e and 8g; wall regions 8b, 8d, 8f and 8h.
Source: elaborated by the authors

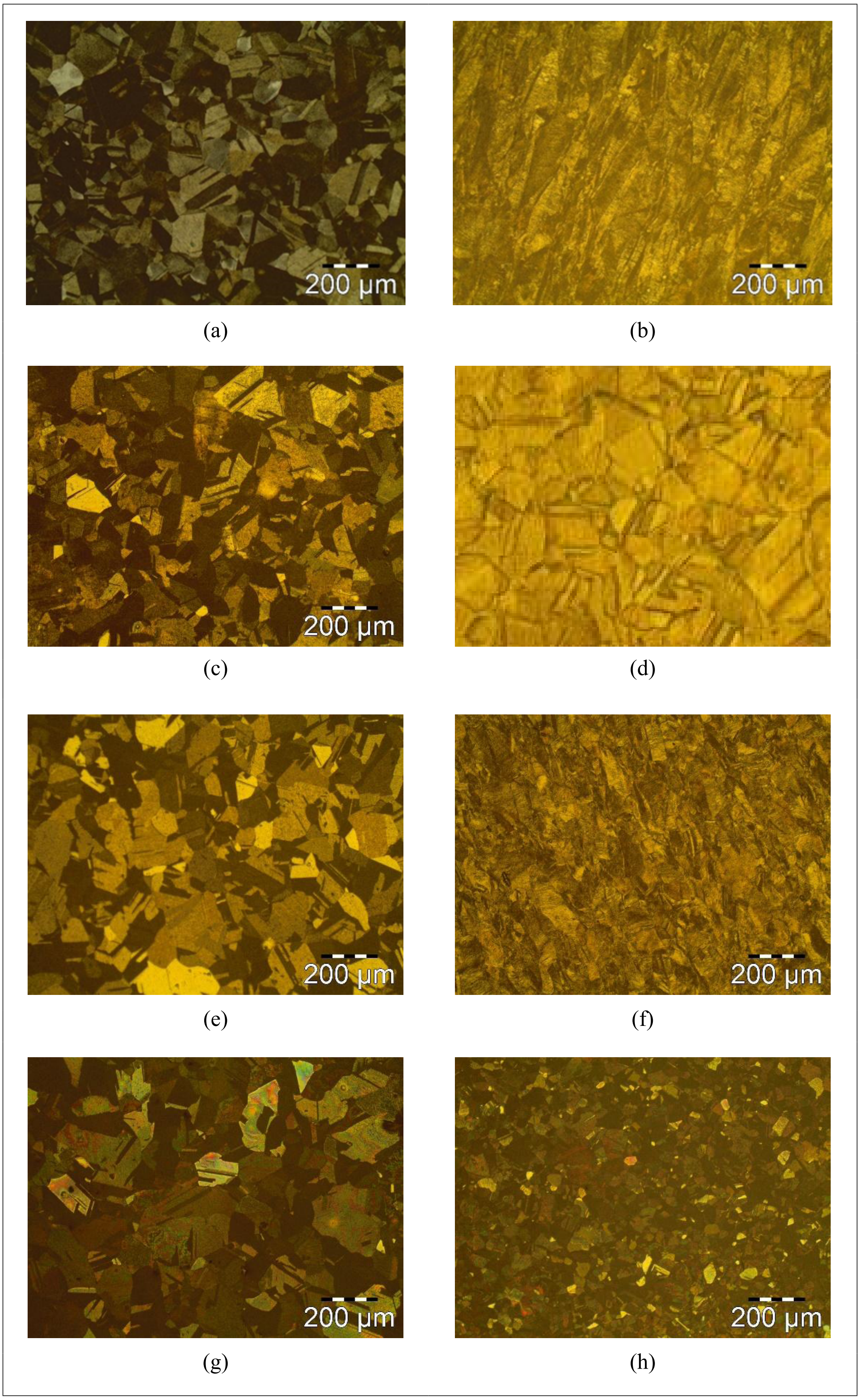

No significant changes were observed in the bottom regions; their microstructure remains similar to that of the original blank. This was expected, due to the minimal dimensional change in that area, which indicates negligible mechanical deformation. Conversely, the wall regions exhibit evident microstructural evolution during forming, distinguishing them from the original blank. In Figures 8b and 8f, elongated grains with corrugated boundaries and intersecting slip bands, typical features of cold strain hardening, are observed. Ozgowicz, Kalinowska-Ozgowicz and Grzegorczyk (2010) reported similar microstructural features in rolled C260 brass with reductions between 15.8% and 70.2%. Crystallographic texture development is also evident, arising from the alignment of the crystallographic axes relative to the macroscopic deformation directions.

The metallographic analysis referring to the thermal annealing treatments (Figures 8d and 8h) reveal smaller isomorphic grains, indicating that there was a significant recrystallization with grains migrating to high-angle boundaries as a result of a diffusion process at high temperatures. Klein and Indacochea (2016), working with 70/30 brass with different %CW and different annealing times and temperatures, found similar microstructures with variables similar to that of this work and attributed the small grains sizes to the high cold deformation index. Ozgowicz, Kalinowska-Ozgowicz and Grzegorczyk (2010) also reported a similar relationship in their work.

The grain size of the blank and of the samples submitted to the thermomechanical processing followed a Gaussian distribution, which allowed for the application of Tukey's test to compare their average grains sizes, using Rstudio software. Table 3 represents the mean grain size values obtained by the Heyn linear intercept method (LIM), along with the corresponding ASTM grain size number (G).

Table 3 ▶
Average Grain Size and G (ASTM) values.
Source: research data

Operation	Bottom Region		Wall Region	
	λ (μm)	G (ASTM)	λ (μm)	G (ASTM)
Blank	47.36	5	47.36	5
Deep Drawing	53.27	5	52.06	5
1st Annealing	51.01	5	26.32	7
Stretch forming	44.88	6	44.21	6
2nd Annealing	53.27	5	31.07	7

The average grain size values for the bottom region showed slight changes in grain sizes during the sequence of operations which, after being compared by Tukey's test, proved to be insignificant at a 95% confidence level. Regarding the annealing steps, the lack of significant alteration confirms the first law of recrystallization, which states that a minimum degree of deformation is necessary for it to occur, considering that the energy stored in the material is important to sustain the growth of a nucleus. Klein and Indacochea (2016) did not observe significant changes in the grain structure when annealing a brass without initial deformation for 60 min at 425 °C.

According to Tukey's test, the grain size changes in the wall region after deep drawing and stretching were significant, which is consistent with the high degree of cold work imposed during these operations. It should be clarified that this reduction is not grain coarsening but the formation of a new deformation-induced microstructure, typical of low stacking-fault-energy materials in which mechanical twinning and dislocation glide elongate grains and produce parallel slip bands. Ozgowicz, Kalinowska-Ozgowicz and Grzegorczyk (2010) reported similar microstructures in rolled C260 brass with approximately 42.5% reduction. Likewise, recent studies employing strain-gradient samples confirmed that cold-worked α-brass exhibited comparable features under subsequent heat treatment (Birchall; Bishop, 2025). Birch *et al*. (2024) obtained closely related results for the same alloy.

ISSN 2447-9187

Observations of grain size in the wall region after annealing (first and second) indicate a significant decrease, as confirmed by Tukey's test. This suggests that the annealing process provided sufficient thermal energy to facilitate dislocation movement, relieve deformation-induced stresses, and promote the nucleation of new grains. Klein and Indacochea (2016) investigated the effects of variables such as %CW, temperature, and time on the recrystallization behavior of C260 brass. He found that during recrystallization, the material's microstructure resembles its pre-worked state in shape, with grain size varying depending on these factors. Similar findings were reported by Moreira, Cruz and Oliveira (2023) and Nascimento, Cruz and Oliveira (2023).

Another noteworthy observation is that the smallest grain size occurs after the first annealing following the operation with the highest percentage of cold work (deep drawing) and also when compared to stretching, as confirmed by Tukey's test, indicating a highly significant change. This aligns with the fourth law of recrystallization, which states that a higher degree of deformation produces smaller recrystallized grains, since more intense deformation generates higher number of nuclei per unit volume, resulting in a smaller average grain size (Humphreys; Hatherly, 2004). Aniceto *et al*. (2016) evaluated C260 brass laminated from an initial to a final thickness through two pass schedules and observed that the sample with fewer rolling passes exhibited higher nucleation intensity during recrystallization under the same temperature and annealing time, producing a smaller average grain size compared to the sample with more passes. Figure 9 illustrates the microhardness measurements along the test specimens.

Figure 9 ▶
Evolution of Vickers microhardness during the manufacturing process.
Source: elaborated by the authors

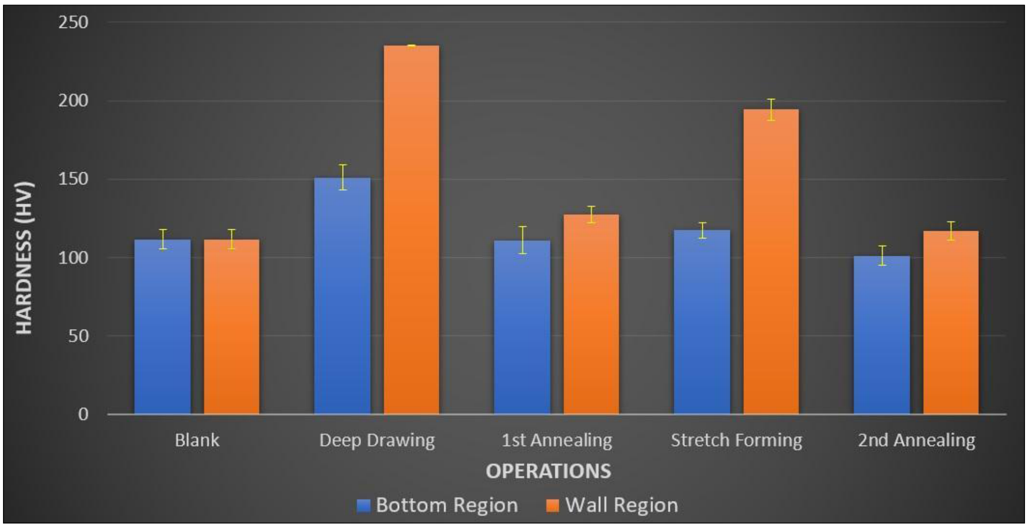

Similar to the grain size analysis, the hardness profile of the bottom region shows little variation across the stages. Although increases in hardness were observed after deformation operations and decreases after annealing, the differences between consecutive steps remain small. The only value that stands out significantly is that of the post-drawing specimen, which exhibits the highest hardness in this region. This behavior was expected, considering that, although thickness changes are minimal at the bottom, there is a visible geometric modification when comparing the curvature radius of the blank with that of the bottom after the operation. Brooks (1982) explains that metals with low stacking fault energy exhibit low dislocation mobility, a condition that significantly reduces the occurrence of climb and cross-slip phenomena. Moreira (2015) also emphasizes their effect on dislocation distribution, supporting the fact that alloys with low stacking fault energy, such as brass, tend to accumulate a higher dislocation density, which facilitates hardening and consequently increases material hardness.

Sousa (2014) observed that cold-rolled C26800 brass and C12000 copper exhibited different work hardening behaviors. Brass showed an 80% increase in hardness, while copper showed a 60% increase. Notably, after 30% deformation, copper's hardening rate decreased, whereas brass maintained a more consistent hardening rate. These differences are attributed to the materials' stacking fault energy (SFE): brass has a lower SFE, leading to more uniform dislocation distribution and less dynamic recovery, while copper's higher SFE allows for more dynamic recovery and less dislocation accumulation.

The characteristics discussed above are also observed in the wall region, intensified by the higher %CW, which causes significant variations to occur in its hardness profile that follow the logic already observed in the grain size analysis of this region: hardness increases during post-forming mechanical operations such as deep drawing and stretching, that is, in hardened materials. Values such as 142 HV for a cold rolling reduction of 15.8% and 212 HV for 70.2% were found by Ozgowicz, Kalinowska-Ozgowicz and Grzegorczyk (2010) when working with the same alloy, in accordance with the tests with a view to the highest value of hardness found to be 235 HV in deep drawing while 194 HV after stretching. The hardness behavior also reduced with the recrystallization of the materials, that is, after the respective annealings. This drop in hardness after heat treatment is also consistent with the observations of Mutlu *et al*. (2023), whose study showed that the hardness of the formed material progressively decreased with increasing recrystallization temperature, approaching the initial values at 550 °C.

It is noteworthy that the hardness values between annealing stage have similar values if the respective standard deviations are considered. This fact is also demonstrated in the comparison of the respective grain sizes, which presented an insignificant difference. The fifth law of recrystallization states that to complete recrystallization at the same time and temperature with a larger initial grain, a higher %CW is required. Therefore, the high %CW value in the deep drawing after a larger blank grain size against a lower %CW value in a smaller grain size (from 47.36 μm in the blank to 26.32 μm in the 1st annealing). Such a law could explain such close hardness, but for that it would be necessary to study the kinetics of the recrystallization of the material under these deformation conditions. Furthermore, the grain sizes obtained in the wall regions after annealing were significantly smaller than those of the blank, likely due to the high %CW value of the respective forming steps preceding the heat treatments. Consequently, the hardness values after annealing, despite having been reduced in relation to their respective conformations with efficiency, are still higher than those of the blank.

Another observed fact regarding the hardnesses in the wall region after annealing is that it remains higher than that of the bottom regions of the same samples, even when considering standard deviations. There is a significant grain size difference between these regions within the same samples, which can be explained by the first law of recrystallization. Therefore, the grain sizes of the wall samples in question are smaller than those of the respective bottom regions, which explains their superior hardness. Barbosa (2018) observed this relationship between grain size and hardness when evaluating 70/30 brass after annealing heat treatment. A decrease in hardness with increasing grain size was also reported by Muhammed, Abed and Mustafa (2012) when studying the effects of recrystallization temperature on the mechanical properties of the same alloy. Birch *et al*. (2024) also reported similar hardening behavior in cold-worked α-brass subjected to heat treatment.

5 Conclusions

The annealing stages revealed differences between the bottom and wall regions of the cups. The bottom regions exhibited minimal microstructural and hardness variation, remaining similar to the initial material, which indicates insufficient cold work for recrystallization. In contrast, the wall regions underwent effective recrystallization during both annealing stages, resulting in significantly smaller equiaxed grains and reducing hardness. The smallest grain size was observed after the first annealing, highlighting the importance of the initial cold work percentage (%CW) in determining the final grain size. This suggests that the %CW during the blank's rolling was lower than in subsequent forming operations, as the annealed grains were notably smaller than those in the original blank. Consequently, the hardness of the annealed material was higher than that of the initial blank.

The blank exhibited an equiaxed microstructure without preferential grain orientation, confirming the effectiveness of the supplier's post-rolling annealing in preventing anisotropic behavior, such as earing. This was corroborated by the absence of such defects during the sample collection. Comparisons among the annealed materials showed negligible variation in grain size and very similar hardness values, emphasizing the importance of initial grain size on the final properties of the material.

A detailed study on the thermal cycles of C260 brass, specifically from the perspective of recrystallization kinetics, would be necessary to deepen the understanding of these effects, particularly because the annealing temperatures and dwell times differ between stages. Furthermore, such a study could provide the technical basis for optimizing the manufacturing process under investigation.

5.1 Study limitations and future perspectives

Limitations:

- Dependence on a pre-existing industrial route: the study represents a cross-section of a consolidated manufacturing process. Consequently, it was not possible to modify certain variables, such as the specific percentages of cold work at each stage.
- Restriction to the use of existing dies: the dies employed in forming were pre-existing and could not be replaced, either due to the high manufacturing cost or the requirement to maintain fidelity to the actual industrial process.
- Limitation regarding the alloy: the C260 brass (70/30) is the established material for cartridge manufacturing, which prevented its comparison with alternative alloys in this study.
- High material cost: the considerable value of brass limited the acquisition of a larger number of samples, restricting the experimental scope.

Future Perspectives:

- Expansion of the experimental base: seek institutional or industrial partnerships to increase material availability, enabling a broader range of tests and greater statistical robustness.

- Conduct studies on the recrystallization kinetics of C260 brass under different levels of cold deformation and annealing conditions (time/temperature), aiming to model the mechanisms of grain nucleation and growth;
- Employ advanced characterization techniques (MEV, EBSD, TEM) to map crystallographic texture, twin distribution, and low/high-angle grain boundaries, enabling the correlation between microstructure and mechanical properties on a more detailed scale;
- Perform computational simulations of the alloy's behavior during forming and annealing cycles to predict microstructural evolution and optimize industrial processes.

Funding

This research received no financial support.

Conflicts of interest

The authors declare no conflict of interest.

Note

The results presented in this study are derived from the undergraduate thesis of Douglas Luiz da Cruz for the Bachelor's Degree in Metallurgical Engineering at the Federal Institute of Education, Science and Technology of Southeast Minas Gerais (IF SUDESTE MG) – Juiz de Fora Campus, available at: https://drive.google.com/file/d/1qQ9qpMYpQrypBNSYtqABpJ_B08MXKkKU/view?usp=sharing. (access available upon reader request).

Authors' contributions

CRUZ, D. L.: conceptualization or study/research design; data collection, analysis, and/or interpretation; writing and preparation of the original draft; **OLIVEIRA, M. J. C.:** writing and preparation of the original draft; critical review with significant intellectual contribution; general supervision and project coordination; **MEINHARDT, C. P.:** critical review with significant intellectual contribution. All authors participated in the writing, discussion, reading, and approval of the final manuscript.

References

ANICETO, P. J.; AMEIDA, L.; TRESSIA, G.; MOREIRA, V. C.; PACHECO, M. T. T. Avaliação da influência do caminho de laminação no tamanho de grão final. *In*: SEMINÁRIO DE LAMINAÇÃO, 53., 2016, Rio de Janeiro. **Anais** [...]. Rio de Janeiro: ABM, 2016. p. 340-347. DOI: https://doi.org/10.5151/1983-4764-27820. In Portuguese.

ASM INTERNATIONAL. **ASM Handbook Volume 2**: Properties and Selection: Nonferrous Alloys and Special-Purpose Materials. Novelty, OH: ASM International, 1992. ISBN 978-0-87170-378-1. DOI: https://doi.org/10.31399/asm.hb.v02.9781627081627.

ASTM INTERNATIONAL. **ASTM E112-10**: Standard test methods for determination average grain size. West Conshohocken, PA: ASTM International, 2010.

ASTM INTERNATIONAL. **ASTM E3-11**: Standard guide for preparation of metallographic specimens. West Conshohocken, PA: ASTM International, 2017.

BARBOSA, C. Avaliação das características microestruturais da liga cobre-30%zinco após tratamento térmico. *In*: CONGRESSO ANUAL DA ABM, 73., 2018, São Paulo. **Anais** [...]. São Paulo: ABM, 2018. p. 21-30. DOI: https://doi.org/10.5151/1516-392X-31157. In Portuguese.

BARBOSA, C. **Metais não ferrosos e suas ligas**: microestruturas, propriedades e aplicações. Rio de Janeiro: E-papers, 2014. Available at: https://www.e-papers.com.br/produto/metais_nao_ferrosos_e_suas_ligas/?v=dc634e207282. Accessed on: 29 June 2026. In Portuguese.

BIRCH, J.; JENKINS, E.; VRETTOU, A.; SAID, M.; VASHISHTHA, H.; CONNOLLEY, T.; BROOKS, J.; COLLINS, D. M. A micromechanical study of heat treatment induced hardening in α-brass. **Acta Materialia**, v. 278, 120277, 2024. DOI: https://doi.org/10.1016/j.actamat.2024.120277.

BIRCHALL, F.; BISHOP, C. High-Throughput Quantification of Recrystallization Parameters for Alloy Development. **Metallurgical and Materials Transactions A**, v. 56, n. 8, p. 3095-3110, 2025. DOI: https://doi.org/10.1007/s11661-025-07822-4.

BROOKS, C. R. **Heat treatment, structure and properties of nonferrous alloys**. Novelty, OH: ASM International, 1982. ISBN 978-0871701381.

GRIGORAS, C. C.; ZICHIL, V.; CIUBOTARIU, V. A.; COSA, S. M. Machine Learning, Mechatronics, and Stretch Forming: A History of Innovation in Manufacturing Engineering. **Machines**, v. 12, n. 3, 180, 2024. DOI: https://doi.org/10.3390/machines12030180.

HIRT, G.; JUNK, S.; BAMBACH, M.; CHOUVALOVA, I.; AMES, J. **Flexible CNC incremental sheet forming**: process evaluation and simulation. v. 12. Saarbrücken: Institute of Materials Technology/Precision Forming (LWP), Saarland University, 2005.

HUMPHREYS, F. J.; HATHERLY, M. **Recrystallization and related annealing phenomena**. 2. ed. Oxford: Elsevier, 2004. DOI: https://doi.org/10.1016/B978-0-08-044164-1.X5000-2.

KLEIN, J.; INDACOCHEA, J. E. **Recrystallization Behavior of 70/30 Brass**. CME 470 – Physical and Mechanical Properties of Materials. Chicago: University of Illinois, 2016. Available at: https://www.academia.edu/21283133/Recrystallization_Behavior_of_70_30_Brass. Accessed on: 29 June 2026.

MERAYO, D.; RODRIGUEZ-PRIETO, A.; CAMACHO, A. M. Topological Optimization of Artificial Neural Networks to Estimate Mechanical Properties in Metal Forming

Using Machine Learning. **Metals**, v. 11, n. 8, 1289, 2021. DOI: https://doi.org/10.3390/met11081289.

MOREIRA, C. E. S.; CRUZ, D. L.; OLIVEIRA, M. J. C. Aplicação do planejamento fatorial e análise de superfície de resposta no processo de recristalização da liga C260 após estiramento. *In*: CONGRESSO ANUAL DA ABM – INTERNACIONAL, 76., 2023, São Paulo. **Anais** [...]. São Paulo: ABM, 2023. DOI: https://doi.org/10.5151/2594-5327-39612. In Portuguese.

MOREIRA, V. C. **Efeito do teor residual de Fe no recozimento do latão 70/30**. 2015. Dissertação (Mestrado em Engenharia Metalúrgica e de Materiais) – Departamento de Engenharia Metalúrgica e de Materiais, Escola Politécnica da Universidade de São Paulo, São Paulo, 2015. DOI: https://doi.org/10.11606/D.3.2016.tde-22072016-161729. In Portuguese.

MUHAMMED, A.; ABED, A.; MUSTAFA, M. A. Effects of recrystallization temperature on the mechanical properties of CuZn30 alloy. *In*: NATIONAL CONFERENCE FOR ENGINEERING SCIENCES, 1., 2012, Baghdad. **Proceedings** […]. Baghdad: IEEE, 2012. p. 1-6. DOI: https://doi.org/10.1109/NCES.2012.6740482.

MUTLU, M.; KARAKAŞ, A.; KUŞDEMIR, H.; KOLTAN, U. K.; YALÇINKAYA, T. Flow forming and recrystallization behaviour of CuZn30 alloy. *In*: INTERNATIONAL ESAFORM CONFERENCE ON MATERIAL FORMING, 26., 2023, Kraków. **Proceedings** […]. Millersville: Materials Research Forum LLC, 2023. p. 1021-1028. (Materials Research Proceedings, v. 28). DOI: https://doi.org/10.21741/9781644902479-112.

NASCIMENTO, M. V. S.; CRUZ, D. L.; OLIVEIRA, M. J. C. Análise microestrutural e das propriedades mecânicas da liga de latão 70/30 recozida após embutimento. *In*: CONGRESSO ANUAL DA ABM – INTERNACIONAL, 76., 2023, São Paulo. **Anais** [...]. São Paulo: ABM, 2023. DOI: https://doi.org/10.5151/2594-5327-39623. In Portuguese.

OZGOWICZ, W.; KALINOWSKA-OZGOWICZ, E.; GRZEGORCZYK, B. The microstructure and mechanical properties of the alloy CuZn30 after recrystallization annealing. **Journal of Achievements in Materials and Manufacturing Engineering**, v. 40, n. 1, p. 15-25, 2010. Available at: http://jamme.acmsse.h2.pl/papers_vol40_1/4012.pdf. Accessed on: 29 June 2026.

SOUSA, T. G. **Avaliação de densidade de discordâncias em cobre e latão α deformados por análise de largura de pico de DRX**. 2014. Dissertação (Mestrado em Ciência dos Materiais) – Instituto Militar de Engenharia, Rio de Janeiro, 2014. Available at: https://sucupira-legado.capes.gov.br/sucupira/public/consultas/coleta/trabalhoConclusao/viewTrabalhoConclusao.jsf?popup=true&id_trabalho=443599. Accessed on: 29 June 2026. In Portuguese.